Coupled Magnetomechanical Modeling of Magnetostrictive Materials with Application to Transducer Design

Manik Kumar, Sajan Wahi, Dr. Sushma Santapuri

Department of Applied Mechanics
Indian Institute of Technology Delhi

COMSOL CONFERENCE
2018 BANGALORE

Outline

Outline

Introduction

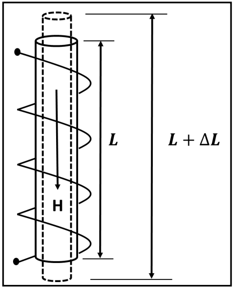

Figure 1: Phenomenon of magnetostrictive materials

- Magnetostrictive Materials are a class of smart materials that exhibits coupling between magnetic and mechanical domains.
- They undergo change in shape when subjected to external magnetic field.

Why their is need for Rare Earth Materials

- Ferromagnets.
  - Low magnetostriction ∼100 ppm.
- Rare earth materials(Terbium, Dysprosium).
  - Low curie point at room temperature.
- Rare earth alloys
  - Terfenol-D ($Tb_xDy_{1-x}Fe_2$)
    - Maximum magnetostriction ∼1250 ppm.
    - Brittle in nature.
  - Galfenol (Fe_xGa_{1-x})
    - Maximum magnetostriction ∼250 ppm.
    - High tensile strength.

Potential Applications of Magnetostrictive Material

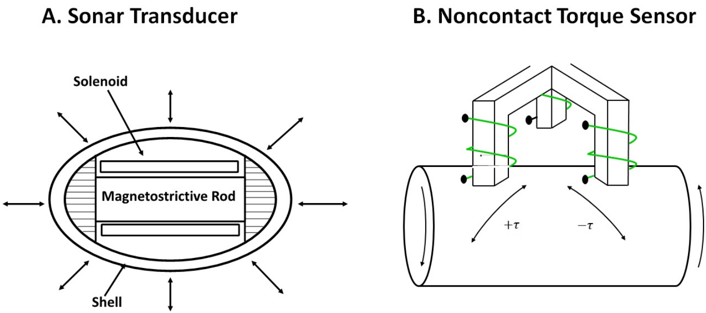

Figure 2: **Applications of magnetostrictive material** [Source: Olabi and Grunwald (2008)]

and many more applications . . .

Outline

Magnetostrictive bending actuator

1. Mudivarthi et al. (2008)
    - Developed 3D Bidirectional Magnetoelastic Model (BCMEM).
    - Computationally expensive model.
2. Graham et al. (2009)
    - Developed 2D Bidirectional Magnetoelastic Model (BCMEM).
    - Compuatationally efficient as compared to Mudivarthi et al. (2008).
3. Cao et al. (2015)
    - Incorporates nonlinear magnetomechanical model.
    - Computationally expensive model.

Outline

Objectives

a. Computationally efficient modeling of magnetostrictive material.
b. Design of magnetostrictive actuator.
   - Computational framework of 2D magnetostrictive rod actuator.
   - Finite element framework for 1D unimoprh bending actuator.

Outline

Energies in Magnetostrictive material

$$\psi(\varepsilon, \mathbf{m}) = \psi_{anisotropy} + \psi_{magnetoelastic} + \psi_{zeeman}$$

where $\mathbf{m}$, ε are the magnetic moment and elastic strain.

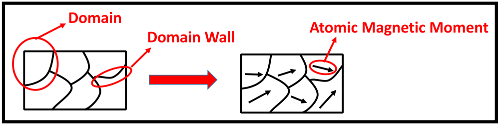

Figure 3: Magnetic domains

$$\psi(\varepsilon, m^k, \xi^k) = \Sigma_k \xi^k (\psi^k_{anisotropy} + \psi^k_{elastic} + \psi^k_{zeeman})$$

where ξ^k is domain volume fraction given by $\dfrac{exp(\frac{-\psi^k}{\omega})}{\sum_{k=1}^{r} exp(\frac{-\psi^k}{\omega})}$.

Locally Linearized Constitutive Model

Constrained Locally Linearized Constitutive Model:
In nonlinear model, a single energy expression is used for any particle orientation whereas in this case a local energy expression is analytically calculated about each easy axis $\boldsymbol{c}^k = [c_1, c_2, c_3]$,

$$\psi_{cons}(m_1, m_2, m_3, L) = \psi_{anisotropy} + \psi_{zeeman} + \psi_{magnetoelastic} + L(m_1^2 + m_2^2 + m_3^2 - 1)$$

Using Taylor series expansion upto second order differential.

$$\frac{\partial \psi_{cons}^k}{\partial m_i^k} = \left.\frac{\partial \psi_{cons}^k}{\partial m_i^k}\right|_{\boldsymbol{c^k}} + \left.\frac{\partial^2 \psi_{cons}^k}{\partial m_i^k m_j^k}\right|_{\boldsymbol{c^k}} (m_j^k - c_j^k) = 0$$

$$[\tilde{\boldsymbol{K}}^k][\boldsymbol{m}^k - \boldsymbol{c}^k] = [\boldsymbol{B}^k]$$

Locally Linearized Constitutive Model (cont.)

Magnetic Induction : $B = \mu_0(H + \sum_{k=1}^{r} \xi^k m^k)$

Total Strain : $S = sT + \sum_{k=1}^{r} \xi^k \lambda^k$

Effect of prestress (σ) on nature of B-H curves

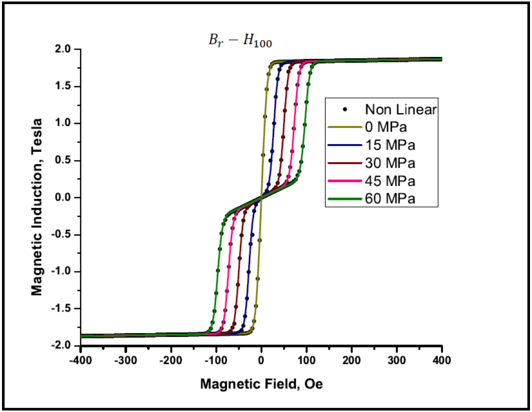

Figure 4: Comparison of magnetic induction (B) vs magnetic field (H) between the nonlinear and locally linearized model along [100] at various prestress values.

Effect of prestress (σ) on nature of λ-H curves

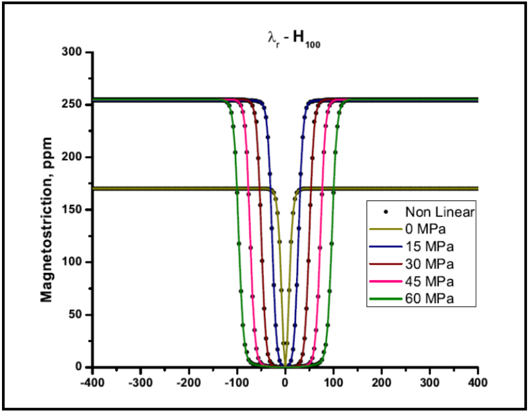

Figure 5: Comparison of magnetostriction (λ) vs magnetic field (H) between the nonlinear and locally linearized model along [100] at various prestress values.

Effect of magnetic field (H) on nature of B-σ curves

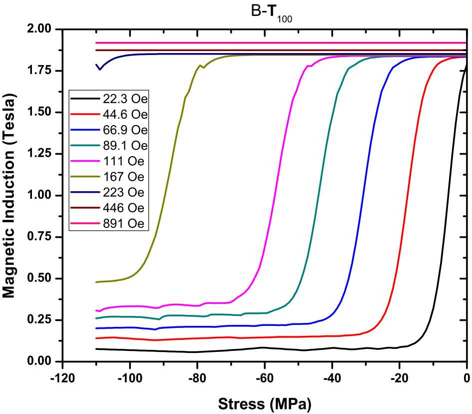

Figure 6: Magnetic Induction (B) vs stress (σ) along [1 0 0] at various prestress values

Effect of magnetic field (H) on nature of ε-σ curves

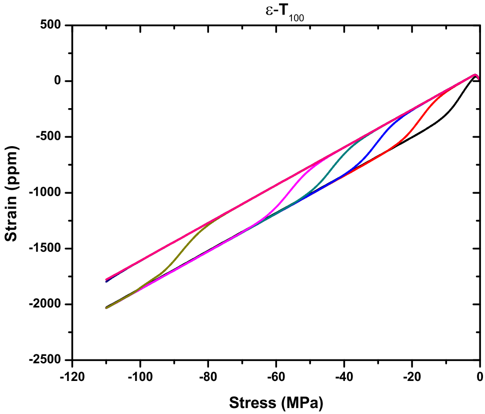

Figure 7: Strain (ε) vs stress (σ) along [1 0 0] at various prestress values

Effect of stress

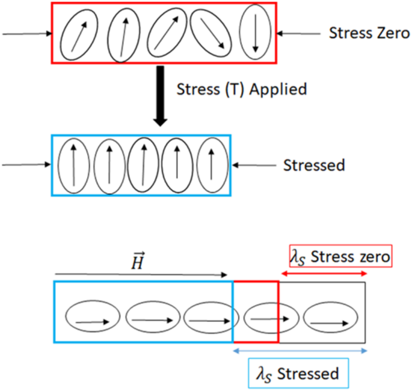

Figure 8: Effect of stress (σ) on magnetization and magnetostriction

3D Magnetomechanical Governing Equations

General constitutive modelling of magnetostrictive materials involves coupling between the magnetic and mechanical BVPs.

Navier's equation in weak form is given by

$$\int_V \left[\mathbf{T} \cdot \delta\,\mathbf{S} + \rho \frac{\partial^2 \mathbf{u}}{\partial t^2} \cdot \delta\mathbf{u} + c \frac{\partial \mathbf{u}}{\partial t} \cdot \delta\mathbf{u} \right] dV = \int_{\partial V} \mathbf{t} \cdot \delta\mathbf{u}\, d\partial V + \int_V \mathbf{f}_B \cdot \delta\mathbf{u}\, dV$$

Also, the magnetostatic governing equation in weak form valid in the magnetic material medium and the surrounding free space is given by

$$\int_{\mathcal{E}} \text{grad}\delta\phi \cdot \mathbf{B}\, dV = 0 \qquad (1)$$

Outline

Applications of Transducer Design

- Applications of transducer

1. 2D axisymmetric rod actuator.
2. Composite unimorph bending actuator.

2D Axisymmetric Transducer Design

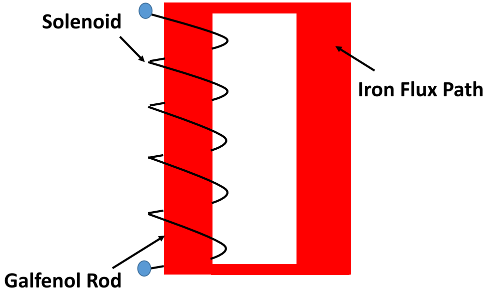

Schematic view of Galfenol rod actuator

Given Current Density, J_0 → Evaluate Magnetic Field, H → Input Magnetization, M using MATLAB function → Compute Magnetic Induction, B $B = \mu_0(M + H)$

Finite Element Solution of Magnetic Boundary Value problem in COMSOL

Outline

Rod Actuator Characteristics

A. Magnetic Flux Distribution

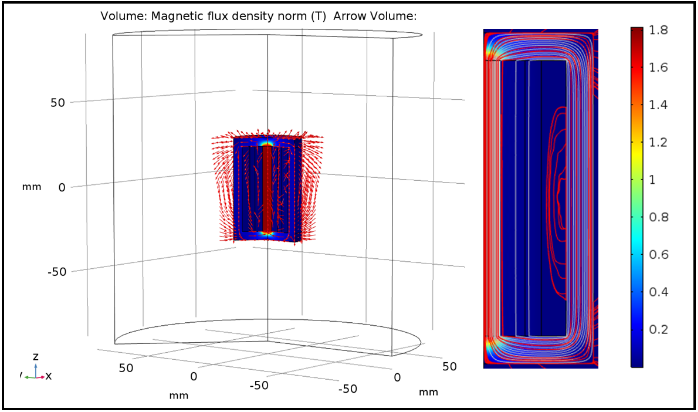

Figure 9: 3D of the norm of magnetic flux density

Rod Actuator Characteristics (cont.)

B. Strain Distribution

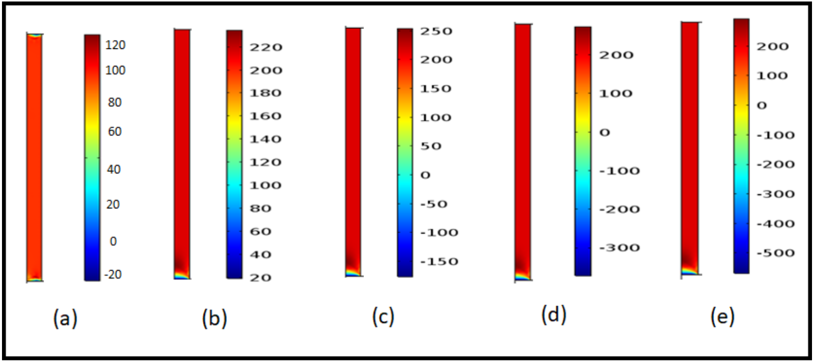

Figure 10: Axial strain distribution at various prestress values in Galfenol rod (a) 0 MPa, (b) 15 MPa, (c) 30 MPa, (d) 45 MPa, (e) 60 MPa

Rod Actuator Characteristics (cont.)

1. Magnetostriction ($\boldsymbol{\lambda}$)-Current Density (J_0)

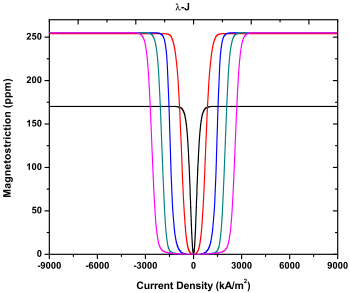

Figure 11: Magnetostriction (λ) vs current density (J_0) for anhysteretic model at various pre-stress values.

Rod Actuator Characteristics (cont.)

2. Magnetic Induction (B)-Current Density (J_0)

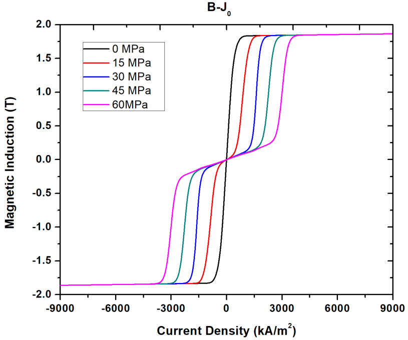

Figure 12: Magnetic induction (B) vs current density (J_0) for anhysteretic model at various pre-stress values.

Composite Unimorph Transducer

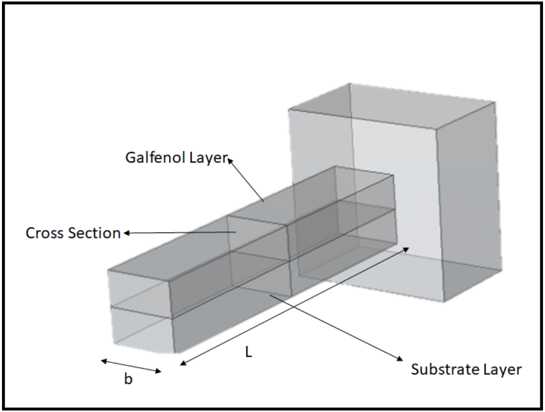

Figure 13: Cantilevered composite magnetostrictive unimorph

Composite Unimorph Transducer (cont.)

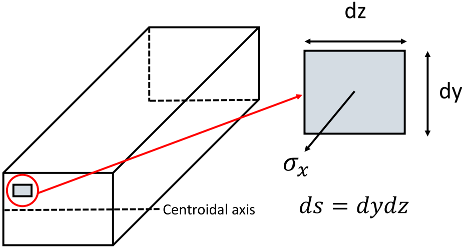

Figure 14: Beam cross-section

Weak form expression of 1D Euler-Bernoulli Beam

$$\int_0^L \left(\frac{d\hat{u}_x}{dx} N + \frac{d\hat{u}_y^2}{dx^2} M\right) dx = 0$$

Composite Unimorph Transducer (cont.)

$$\begin{Bmatrix} N \\ M \end{Bmatrix} = \begin{bmatrix} E_{\text{effective}} A_{\text{effective}} & b(E_{al}\frac{t_2^2}{2} - E_g\frac{t_1^2}{2}) \\ b(E_{al}\frac{t_2^2}{2} - E_g\frac{t_1^2}{2}) & E_{\text{effective}} I_{\text{effective}} \end{bmatrix} \begin{Bmatrix} \varepsilon_0 \\ \kappa \end{Bmatrix} + \begin{Bmatrix} -E_g A_g \lambda \\ E_g b \frac{t_1^2}{2} \lambda \end{Bmatrix}$$

$$E_{\text{effective}} = \frac{(E_g A_g + E_{al} A_{al})}{(A_g + A_{al})},$$

$I_{\text{effective}} = I_g + I_{al} + A_g(\frac{t_1}{2})^2 + A_{al}(\frac{t_2}{2})^2$, and $A_{\text{effective}} = A_g + A_{al}$

Bending Actuator Characteristics

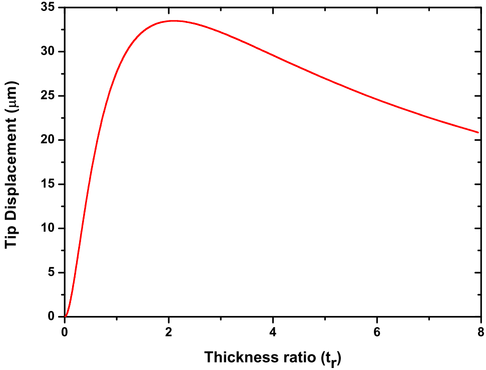

Figure 15: Tip displacement of cantilevered Galfenol-Aluminium unimorph

Bending Actuator Characteristics (cont.)

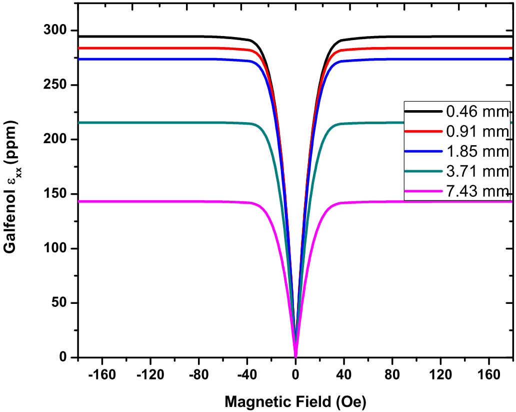

Figure 16: Free strain (ε_{xx}) on Galfenol surface

Bending Actuator Characteristics (cont.)

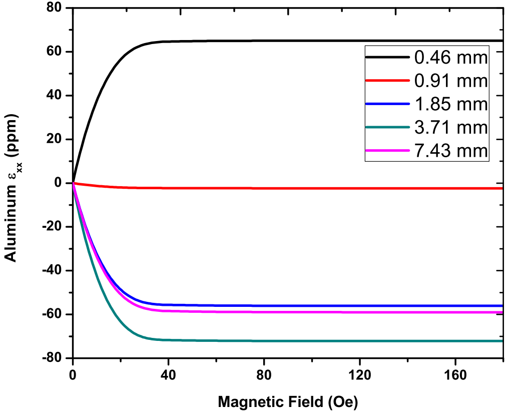

Figure 17: Free strain (ε_{xx}) on aluminum surface

Bending Actuator Characteristics (cont.)

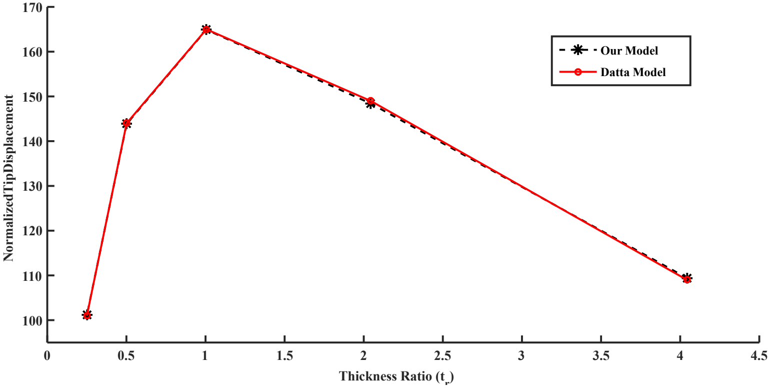

Figure 18: Comparison of normalized tip displacement as predicted by our model and Datta et al. (2008)

References

Armstrong, W. D. (1997). Burst magnetostriction in tb 0.3 dy 0.7 fe 1.9. *Journal of applied physics*, 81(8):3548–3554.

Atulasimha, J. and Flatau, A. B. (2011). A review of magnetostrictive iron–gallium alloys. *Smart Materials and Structures*, 20(4):043001.

Cao, Q., Chen, D., Lu, Q., Tang, G., Yan, J., Zhu, Z., Xu, B., Zhao, R., and Zhang, X. (2015). Modeling and experiments of a laminated magnetostrictive cantilever beam. *Advances in Mechanical Engineering*, 7(4):1687814015573761.

Datta, S., Atulasimha, J., Mudivarthi, C., and Flatau, A. (2008). The modeling of magnetomechanical sensors in laminated structures. *Smart Materials and Structures*, 17(2):025010.

Evans, P. and Dapino, M. (2010). Efficient magnetic hysteresis model for field and stress application in magnetostrictive galfenol. *Journal of applied physics*, 107(6):063906.

References (cont.)

Graham, F., Mudivarthi, C., Datta, S., and Flatau, A. (2009). Modeling of a galfenol transducer using the bidirectionally coupled magnetoelastic model. *Smart Materials and Structures*, 18(10):104013.

Mudivarthi, C., Datta, S., Atulasimha, J., and Flatau, A. (2008). A bidirectionally coupled magnetoelastic model and its validation using a galfenol unimorph sensor. *Smart Materials and Structures*, 17(3):035005.

Olabi, A.-G. and Grunwald, A. (2008). Design and application of magnetostrictive materials. *Materials & Design*, 29(2):469–483.

THANK YOU FOR YOUR PATIENCE
QUESTIONS ?